On the storm runoff process in the Ara experimental basin

By Yasuo ISHIHARA and Shigeki KOBATAKE

Synopsis

Since 1967, detailed observation of hydrological events concerning runoff phenomena of rainfalls has been continued in the Ara experimental basin. This paper consists of the following two parts. The first part is the conversion process from rainfall to runoff in a specified sub-basin, referred to as a unit cell, in the basin. Considering the results of rainfall measurements, running water on and/or through the porous surface layer covering the mountain slope, soil moisture at various depths, seeping water from the crack of the rock, flowing water at the outlet of the sub-basin, and so on, a runoff model having four soil strata for slope process and one stream reach for channel process is proposed, whose parameters are developed from the above analysis and the water balance in the sub-basin. The second part is the formation process of a hydrograph of storm runoff in the stream net of the basin. After dividing the basin into a net of stream channels and a set of unit cells given by ridge lines passing through all confluences of the stream net resulting from the order analysis of a drainage net, it is shown that a stream reach is approximately characterized by a so-called linear channel. Then a hydrograph of storm runoff can be calculated by using a kind of time-area-concentration diagram.

1. Introduction

In order to elucidate the hydrological phenomena with respect to the runoff process and the water balance in a mountainous watershed, first of all, the correct understanding of the hydrological events occuring in the watershed is to be desired. With this in mind, the Ara experimental basin was arranged in 1967 as a part of the scientific project of the UNESCO International Hydrological Decade, at Kyoto University.

The Ara experimental basin is 4.40 km^2 in area, as shown in Fig. 1, and an upstream part of the River Ara, a tributary of the River Yasu flowing into Lake Biwa.

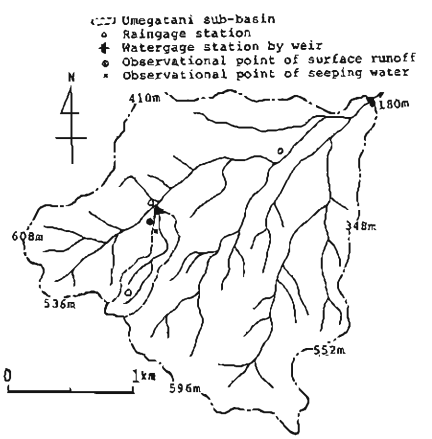

Fig. 1. Topographical outline of the Ara experimental basin.

Furthermore, in order to find out both contributions of the mountain slope and the stream reach to the storm runoff process, the narrow and long shape of watershed, Umegatani sub-basin (0.18 km^2) shown by a dotted line in Fig. 1, was arranged in the experimental basin.

The first part of this paper describes the detailed results of observation obtained in the sub-basin and the runoff model derived by analyzing these results[1)2)3)]. In the second part of the paper, in order to confirm whether the results obtained in a small watershed can be extrapolated to estimate the runoff hydrograph from a large one during a flood, or not, the relation between two flood hydrographs from the Umegatani sub-basin and the whole experimental basin is discussed[4)].

2. Basin characteristics and observations

The experimental basin belongs to the climate region of around 1700 mm in annual rainfall and of 1°C and 27°C in monthly mean temperature in January and August, respectively. The basin is covered densely with both coniferous and deciduous trees, being 60% and 40% in areal ratio, respectively. The surface soil is well-graded sand, weathered granite, ranging 0.2 to 0.4 mm in 10% grain size by weight and 1 to 2 mm in 50% grain size, whose depth reaches several meters. Typical accumulation curves of grain size are shown in Fig. 2.

The inclination angles of mountain slopes and stream reaches range from 25° to 40° and 5° to 15°, respectively. Fig. 3 shows the hypsometric curve of the basin, and, therefore, it is concluded that this basin seems to be at the equilibrium stage of erosion cycle under uniform erosive action.

Usually, the hydrological events concerning the storm runoff, especially in a small watershed, change rapidly with time. It is of importance to take synchronous records of all events. For this purpose, several new instruments for observing the events were developed and a multi-channel recorder of relatively high speed was applied.

The rain gauges employed in the basin are the tipping-bucket type with an accuracy

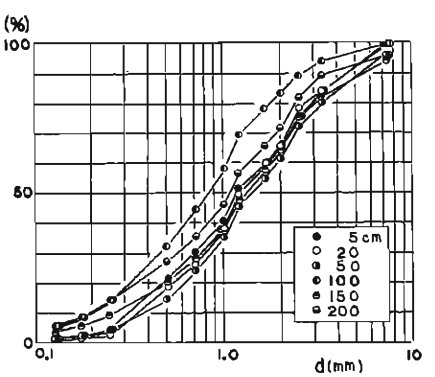

Fig. 2. Accumulation curves of grain size.

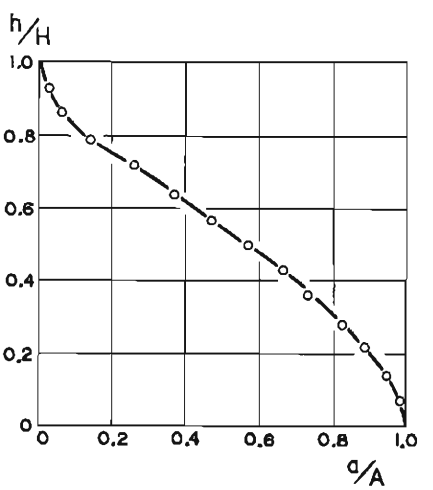

Fig. 3. Hypsometric curve of the basin.

of 0.5 mm and installed at the locations shown in Fig. 1. The observation of discharge rate at the outlet of the Umegatani sub-basin is carried out by converting the changes of a float to the electric signal through a rotary potentiometer, using a concrete weir with 90° V-shaped knotch of 2 m in height. At the outlet of the whole experimental basin, the outflow discharge is measured using a usual broad weir with a water gauge.

3. Results of observation in the sub-basin

In addition to the basic hydrological observations mentioned above, the following hydrological events were measured in the Umegatani sub-basin.

(a) Water flowing on mountain slope

In order to examine the water flow which might appear on a mountain slope during a initial period of rainfall, the water flowing into the trough which was 1 m long and installed horizontally on the slope was measured by the tipping bucket type of flow meter in combination with the rainfall. The location of this instrument is shown in Fig. 1. Fig. 4 shows an example of the results of measurement, in which r is the intensity of rainfall, in mm/min, qs the flowing rate of water measured at the location of 20 m down from the ridge line, in cm³/min, and Q the discharge rate from the sub-basin in l/sec. The flowing water at the location of 10 m down from the ridge line on the slope is also measured simultaneously. It was found out from the results of this observation that:

i) As soon as a rain begins to fall, a very small increment of the discharge at the outlet of the sub-basin is observed because of so-called channel precipitation.

ii) Before the flowing water on the surface soil appears, rainfall of 3–4 mm is needed to make the ground surface and the trees sufficiently wet.

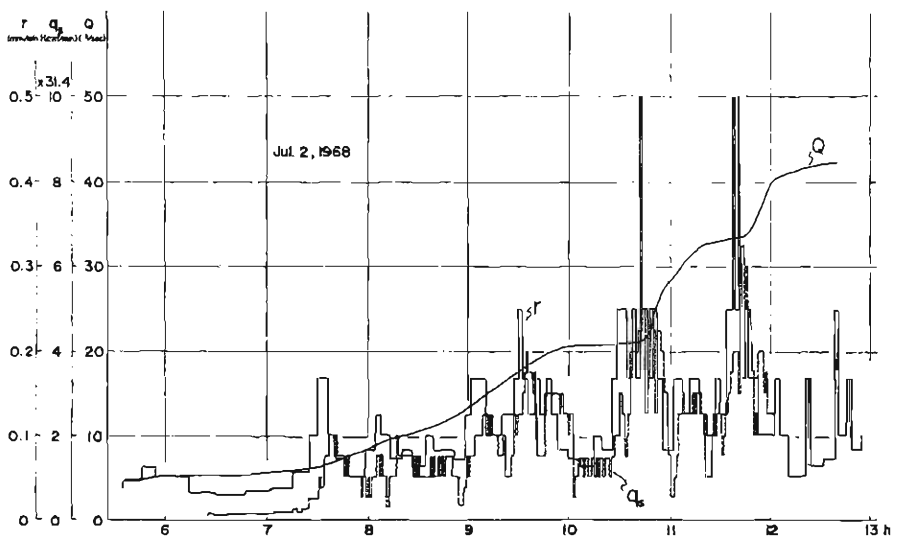

Fig. 4. An example of rainfall and surface flow.

iii) When the intensity of rainfall becomes more than 0.06 mm/min, i.e. 3.6 mm/hr, the amount of the flowing water increases considerably.

iv) The difference between the hyetograph and the hydrograph of the flowing water seems to remain constant, being around 5 minutes in Fig. 4.

From field observation of the surface soil, such flowing water can be understood as a net of small flow running down on the surface of the loose and porous stratum which is composed of short grass and fallen leaves.

(b) Water seeping from a rock fissure

A large granite rock was found in the middle location of the mountain slope shown in Fig. 1. This rock has a fissure from which water is seeping, never drying up at any season of the year. This seeping water seems to be the origin of water supply to the flow in the stream reach of the sub-basin even for periods of no rainfall. Fig. 5 shows the results of measurement of the seeping water by the use of the tipping bucket type of flow meter in combination with the corresponding rainfalls and the hydrograph as the outlet of the sub-basin. In this figure, q represents the amount of seeping water every 1 hour in l/hr, r the rainfall in mm/hr and Q the discharge rate in l/sec. Considering that May is one of dry seasons in this region of Japan, the following characteristics can be determined from this figure:

i) When the discharge rate in the stream reach is relatively small, the seeping water does not increase even after an adequate rainfall, June 1, June 11 and September 30, 1970.

ii) After a large scale rainfall on June 16, and after an adequate rainfall on June 19, June 25 and July 5, the seeping water increased gradually to reach a steady state. The constant value of the seeping water, i.e. steady state appears after 30–40 hours from the beginning of the rainfall and is about 50 l/hr to 70 l/hr, which may be dependent on the antecedent condition of the soil moisture. The constant seeping water continues during a certain period of time.

iii) The very slowly decreasing state of the seeping water follows such steady states. In the decreasing state, the seeping water is proportional to the discharge rate at the outlet of the sub-basin, before June 15, between June 29 and July 5, and after July 9.

(c) Soil moisture

In order to indicate the change of soil moisture, the electric resistance type of moisture meter was installed under the ground near the measuring point of surface flow mentioned in (a). The depths of sensors and gypsum blocks, were 5 cm, 15 cm, 25 cm, 40 cm, 70 cm and 100 cm from the ground surface. The general view of the moisture profile is shown in Fig. 6, in combination with the void ratio of soil at two locations. In this figure, the abscissa represents directly the value of electric resistance, which may be roughly inversely proportional to the soil moisture content, because it is not always possible to measure the soil moisture accurately by the resistance type of soil meter. Figs. 7 (a) and (b) are the detailed change of the moisture profile between July 7 and August 4, 1970, which is picked up from Fig. 6. Fig. 7 (a) shows the drying state for a few rainfalls and (b) shows the wetting state for a shower of 49 mm. The following can be determined from these figures.

i) The soil moisture of the surface stratum from 0 cm to 25 cm in depth varies

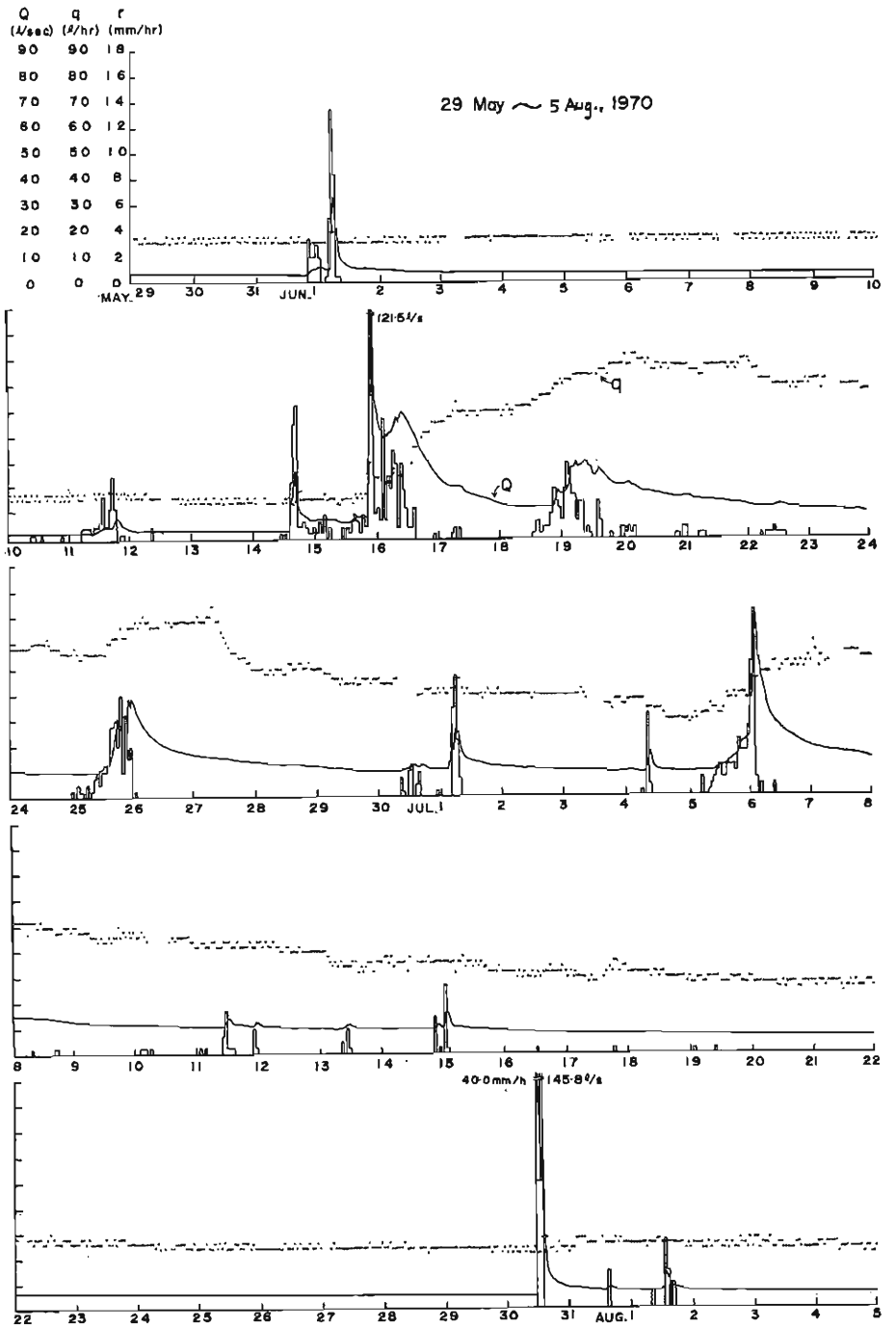

Fig. 5. An example of rainfall, runoff hydrograph and seeping water.

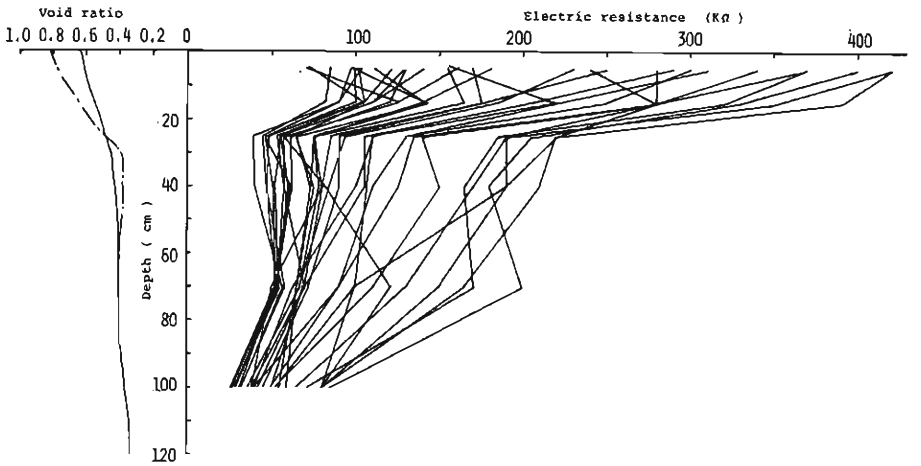

Fig. 6. The general view of the soil moisture profile expressed by electric resistance.

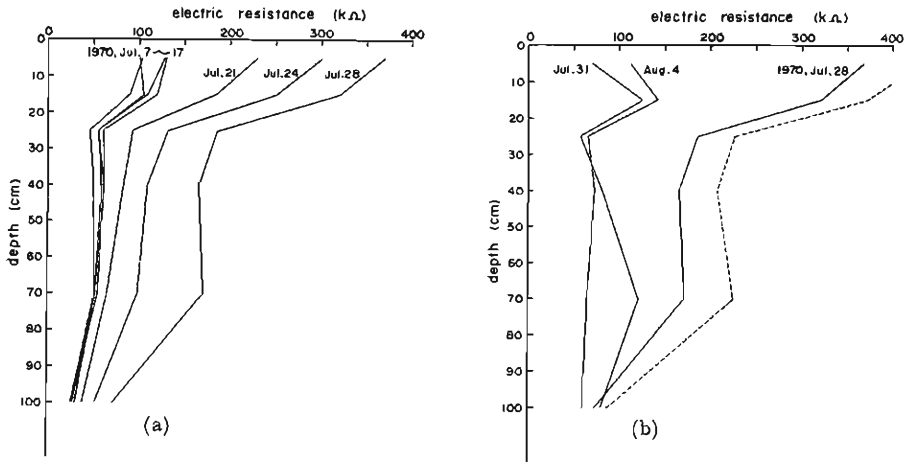

Fig. 7. The soil moisture profile expressed by electric resistance.
(a) July 7–28, 1970.
(b) July 28-August 4, 1970.

very widely and that of the second stratum from 25 cm to 70 cm varies to a lesser degree. On the other hand, the soil moisture of the third stratum below 70 cm in depth varies little and is always wet.

ii) After a rainfall, the rain-water moves down slowly in the soil column and at the same time, the soil moisture begins to decrease from the upper part of the soil column.

4. Physical runoff model of the sub-basin

Based upon the results of the observations presented above, the physical runoff model of the sub-basin can be constituted. In the runoff model, not only the flow

elements in the mountain slope but also the flow in the stream reach must be simulate reasonably.

The situation of the running water on the mountain slope is determined from the measurement of water coming into the trough installed on the slope and it is presumed by the observation of the seeping water from the fissure of the rock that there exists at least three flow elements under the ground surface of the slope. Furthermore, it is not to be doubted from the results of auger boring and the measurement of soil moisture that the mountain slope consists of several kinds of soil layer in the sense of permeability. In the runoff model, therefore, a slope element which consists of four strata as shown by Fig. 8 (a) can be proposed to represent such hydrological events in the actual slope.

The output from the slope element is to become the input for the channel element in the runoff model together with the channel precipitation. The flow in the stream reach, therefore, is characterized by an open channel flow with lateral inflow which is distributed along the channel. Such a channel gives the channel element in the runoff model.

Consequently, the runoff model of the sub-basin can be composed of the channel element and the slope element, which is attached to the channel element and consists of four strata as shown in Fig. 8 (b). In this paper, the process in the slope element, through which a rainfall is transformed into the inflow to the channel element, is called the slope process. Such a process where the water flows down in the channel element, to which the rain falling on the channel and the outflow from the slope element are being supplied as two kinds of lateral inflows, is called the channel process.

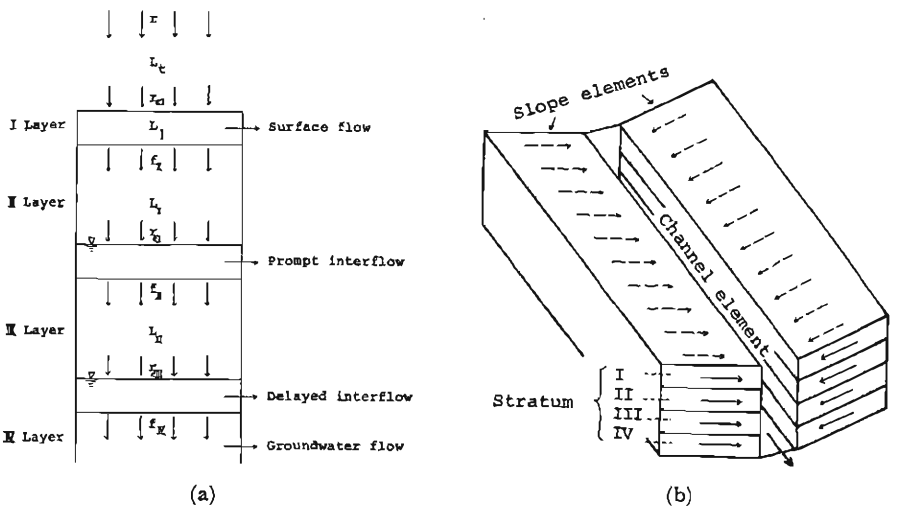

Fig. 8. The runoff model of the Umegatani subbasin

5. Determination of the model parameters

Although the characteristics of the physical factors governing hydrological events

in the actual basin, strictly speaking, varies locally, it seems to be allowable for the purpose of the runoff estimation at the outlet of the Umegatani sub-basin that the length and the gradient of the slope and the thickness of each stratum can be assumed to be constant approximately.

The length of the stream reach in the sub-basin is 1.5 km and there are similar mountain slopes to each other on both sides of the stream reach. Consequently, it is assumed that the sub-basin is simulated by the rectangular model basin composed of a channel element being 1.5 km long and two uniform slope elements being 60 m wide on both sides.

(a) Water balance in the sub-basin and rate of evapotranspiration

The annual precipitation and the total height of runoff in 1970 were 1840 mm and 1160 mm, respectively. Therefore, the annual loss of precipitation resulting in evapotranspiration and basin leakage is estimated as 680 mm, which is the value of the same order as those in many experimental basins in Japan.

The water balance equation for one rainfall event is given by

$$\left[\int_A dA\int_0^{z_0} m\,dz\right]_{t=t_0} - \left[\int_A dA\int_0^{z_0} m\,dz\right]_{t=0} = \int_A dA\int_0^{t_r} r_e\,dt - \int_0^{t_0} Q\,dt - \int_A dA\int_0^{t_0} e\,dt \tag{1}$$

in which A is the drainage area, Z the depth from the ground surface, Z_0 the thickness of soil layer, t the time from the beginning of rainfall, t_r the end time of the rainfall, t_0 the time when the runoff intensity after the rainfall becomes to be equal to that at $t=0$, r_e the rainfall intensity on the soil surface, Q the runoff intensity from the basin, m the soil moisture content being function of Z, e the evapotranspiration rate. It can be assumed approximately that the soil moisture content at $t=t_0$ is equal to that at $t=0$. Therefore, the left side of equ. (1) vanishes. That is,

$$\int_0^{t_r} r_e\,dt - \int_0^{t_0} \frac{Q}{A}\,dt = \int_0^{t_0} \bar{e}\,dt \tag{2}$$

in which $\bar{e}$ is the average evapotranspiration rate over the area. In equ. (2), denoting $r_e=r-r_i$ in which r is the rainfall intensity and r_i the rate of interception including the rainwater necessary to make the ground surface wet, the following relation can be obtained.

$$\int_0^{t_r} r\,dt - \int_0^{t_0} \frac{Q}{A}\,dt = \int_0^{t_r} r_i\,dt + \int_0^{t_0} \bar{e}\,dt \tag{3}$$

The first term of the right side of equ. (3) expresses the total amount of interception and wetting which will disappear by evaporation after the rainfall. This value is considered to be constant for a heavy rainfall[5], because little evaporation occurs during a short period of such a rainfall. The second term of the right side expresses the total amount of evapotranspiration resulting from the increment of soil moisture content and this value will become large according as the increase of (t_0-t_r), if no evapotranspiration is assumed to take place during the rainfall. Therefore, denoting the right side of equ. (3) as EL, EL can be expressed by,

$$EL = a + F(t_0 - t_r)$$

in which a is a numerical constant and $F(t_0-t_r)$ shows the function of (t_0-t_r). Namely, plotting the relation between EL and (t_0-t_r) and drawing the average curve passing through the plotted points, the value of EL at which the curve crosses

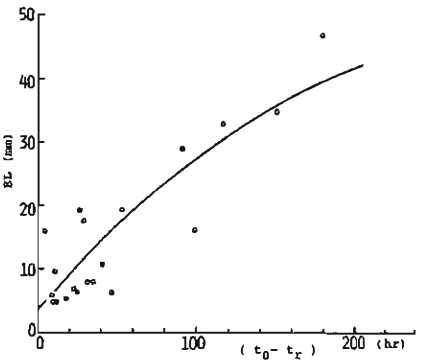

Fig. 9. The relation between EL and (t_0-t_r).

the EL-axis gives the amount of interception including the rainwater to make the ground surface wet and evaporating after the rainfall. Fig. 9 shows relation between EL and (t_0-t_r) obtained for the sub-basin. From this figure, the amount of interception, and wetting is found to be 4 mm.

Considering, moreover, that the rate of evapotranspiration from the ground surface, ET, remains constant, C_0, in the state of the water content exceeding the ordinary one and decreases exponentially with elapsing time in the state of the water content not exceeding the ordinary one, the curve of Fig. 9 can be re-plotted by differentiation as shown in Fig. 10. Denoting the time when the water content of the surface soil has become the ordinary water content as t_c, the following relation is obtained from Fig. 10.

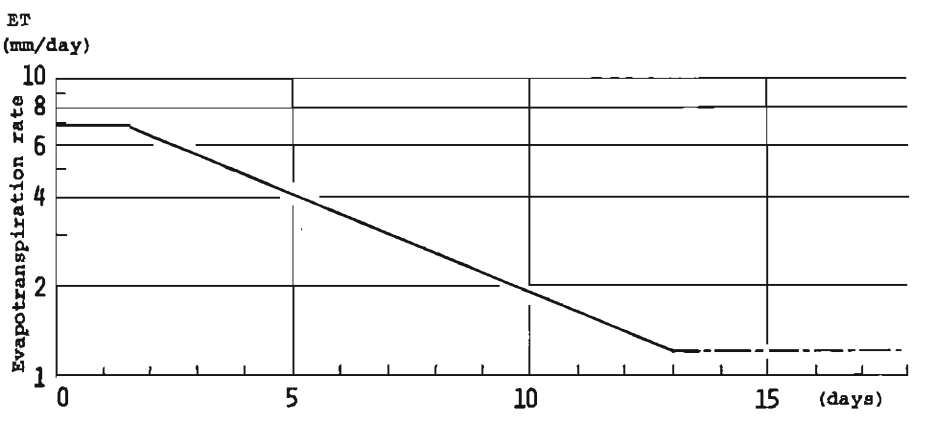

Fig. 10. The relation between ET and (t_0-t_r).

$$\left.\begin{aligned} ET \equiv C_0 = 7 \text{ mm/day}, \quad & \text{for } t_r \leqq t \leqq t_c \\ ET = C_0 e^{-0.15(t-t_c)}, \quad & \text{for } t_c \leqq t, \end{aligned}\right\} \tag{4}$$

in which $t_e - t_r = 1.5$ days and t is in day.

When the value of $t - t_e$ becomes large, the soil moisture reaches equilibrium. In other words, the rate of evapotranspiration from the ground surface becomes equal to the rising rate of water through the underlying soil by capillary action. Fig. 11 shows the relation between the time elapsed after the end of rainfall $t - t_r$, and the electric resistance, representing indirectly the soil moisture, measured at the depth

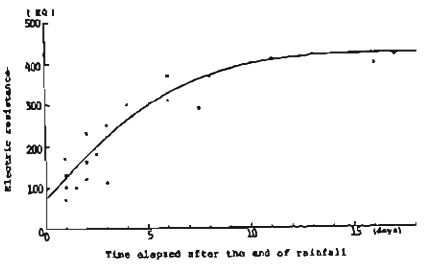

Fig. 11. The change of soil moisture at the depth of 5 cm below the ground surface.

of 5 cm below the ground surface. In this figure, the surface soil moisture seems to remain constant while $t - t_r \geqq 13$ days. It is reasonable, therefore, to assume that the rate of evapotranspiration remains constant for $t - t_r \geqq 13$ days. This assumption is shown by the chain line in Fig. 10 and the constant value is 1.2 mm/day.

(b) Model parameters with respect to the surface stratum

i) Initial retention

The retention, including the interception by trees L_t and the rain-water needed to make the surface stratum sufficiently wet L_I, is estimated to be 4 mm.

ii) Effective rainfall to the surface flow

Such a running water on or through the surface stratum as mentioned in Section 3. (a) is called the surface flow in this paper as shown in Fig. 8. The surface flow is assumed to appear appreciably when the rainfall intensity exceeds 0.06 mm/min (see Section 3. (a), iii)). Moreover, it was found out by comparing the computed hydrographs through the runoff model presented here with the observed ones for the initial duration of runoff increment that 5% of ($r' - 0.06$ mm/min) is the effective water supply to the surface flow, in which r' is the intensity of the rainfall excluding L_t and L_I. The remaining rainfall, $(0.06 \text{ mm/min} + (1 - 0.05)(r' - 0.06 \text{ mm/min}))$, infiltrates into the II-stratum.

iii) Propagation speed with respect to the surface flow

The surface flow is governed by Darcy's law, because this flow is assumed to be a very weak flow passing through the porous surface stratum. Therefore, the following equations are obtained.

$$\gamma_I \frac{\partial h}{\partial t} + \frac{\partial q_I}{\partial x} = r_{eI} \quad \text{and} \quad q_I = v_I \cdot h \tag{5}$$

in which γ_I is the effective porosity of surface stratum, h the apparent water depth, q_I the discharge rate per unit width, v_I the apparent velocity of flow and r_{eI} effective rainfall to the surface flow. From equ. (5), the discharge rate at the end of the slope, q_{I0}, can be obtained easily as follows:

$$q_{I0}=v_I'\cdot\int_{t_1}^{t_2}r_{eI}\,dt \tag{6}$$

in which $v_I'=v_I/\gamma_I$ and t_2-t_1 is the time of propagation from the top of the slope to the end when the speed is assumed to be v_I'. Basing upon the time difference between the peak of rainfall and the one of surface flow which is explained in Section 3. (a), iv), the propagation speed v_I' can be estimated to be 20 m/10 min=10/3 cm/sec.

(c) Model parameters with respect to the II-stratum and the III-stratum

i) Initial loss of rain-water

The prompt interflow and the delayed interflow are assumed to appear in the II-stratum and the III-stratum as shown in Fig. 8. A portion of the rain-water penetrating from the top surface of each stratum is to be stored temporarily in the unsaturated zone of the stratum and to evaporate through the ground surface after the rainfall. Generally speaking, the integration of ET with time gives the quantity of water to be stored, that is, the initial loss of rain-water. Assuming that the water to evaporate from the ground surface is supplied from the II-stratum for the duration between $t-t_r=0$ and 6.5 days when the change of electric resistance at 5 cm below the ground surface becomes small as shown in Fig. 11 and from the III-stratum for the duration between $t-t_r=6.5$ days and 13 days, the maximum value of the initial loss of rain-water becomes 35.1 mm for the II-stratum and 14 mm for the III-stratum. Denoting the time interval from the end of the antecedent rainfall to the beginning of the rainfall under consideration as t_a, when $t_a\leqq 6.5$ days, the initial loss of the rain-water in the II-stratum, L_{II}, is given by integrating the ET-curve of Fig. 10 from $t=0$ to t_a and, when 6.5 days$\leqq t_a\leqq$13 days, L_{II} becomes its maximum value of 35.1 mm and L_{III} is given by integration from $t=6.5$ days to t_a.

ii) Supplying rate of rain-water to the prompt interflow and the delayed interflow

The supplying rate of rain-water to the prompt interflow can be given easily as the remaining rainfall after removing the initial loss, L_{II}, in the II-stratum from $f_{II}=(0.06\text{ mm/min}+(1-0.05)(r'-0.06\text{ mm/min}))$. So, the effective rain-water to the prompt interflow is given as $r_{eII}=f_{II}-f_{III}$.

The infiltration rate of water into the III-stratum is governed by the water content in its top zone. Although, usually, the infiltration rate of water is described by the Horton's equation of infiltration capacity, it is assumed here for simplicity that the infiltration rate of water, f_{III}, decreases linearly with time when the total amount of infiltrated water equals the maximum value of L_{III} and, after that time, remains constant, and that the rain-water begins to be supplied to the delayed interflow at that time. This relationship is shown in Fig. 12, in which f_{IIIm} is the maximum rate of infiltration to the III-stratum and is assumed as 0.06 mm/min=3.6 mm/hr, referring to the value at which the surface flow occurs. L_{III} gives the amount of rain-water lost before the delayed interflow appears. The constant value, f_{IIIc}, being equal to the water supply to the delayed interflow in the III-stratum, can be determined from the results of measurement of the seeping water from the aforementioned rock fissure. The maximum and constant rate of the seeping water is 70 l/hr and the ratio of the rate of seeping water to the discharge rate at the outlet of the sub-basin during a long term of no rainfall is 1/940. Therefore, assuming that both the

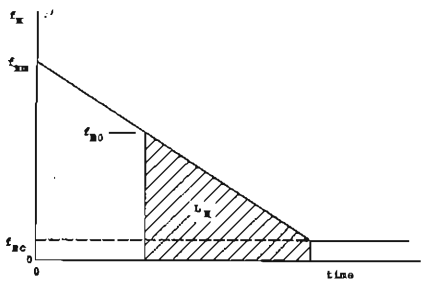

Fig. 12. The infiltration curve used in the runoff model.

delayed interflow and the groundwater flow appear over the whole slope and that this ratio remains unchanged while the delayed interflow occurs in company with the groundwater flow, the constant rate of water supply to the delayed interflow, f_{IIIe}, is estimated to be 0.36 mm/hr. So, the effective rain-water to the delayed interflow is given as $r_e=f_{\text{IIIe}}-f_{\text{IV}}$.

iii) Propagation speeds of the prompt and delayed interflows

It is obvious that the same kind of equation as equ. (5) is satisfactory for each interflow. The average velocity, v_{II} or v_{III}, can be expressed by $K_{\text{II}}\cdot\sin\theta$ or $K_{\text{III}}\cdot\sin\theta$, in which K_{II} or K_{III} is the coefficient of permeability and θ the inclination angle of the slope.

Basing upon the fact that the time of around 35 hours is needed until the delayed interflow reaches a steady state as seen in Fig. 5, the propagation speed for the delayed interflow, $K_{\text{III}}\cdot\sin\theta/\gamma_{\text{III}}$, is estimated to be 0.023 cm/sec. On the other hand, the porosity of the soil at 60 cm below the ground surface is measured to be $\gamma_{\text{III}}=0.4$ by auger boring and the value of $\sin\theta$ is assumed to be 0.64. Therefore, the value of K_{III} is calculated to be 0.014 cm/sec. Next, assuming that the coefficient of permeability is proportional to the square of the 10% grain size by weight, the value of K_{II} can be estimated as $K=0.014\times(0.04)^2/(0.025)^2=0.035$ cm/sec, in which the values of 0.04 and 0.025 are the 10% grain sizes of the II-stratum and the III-stratum in cm, respectively. Consequently, the propagation speed for the prompt interflow, $K_{\text{II}}\cdot\sin\theta/\gamma_{\text{II}}$ is estimated to be 0.041 cm/sec.

(d) Model parameters with respect to the groundwater flow

The maximum value of the seeping water resulting from the groundwater flow seems to be 30 l/hr, for example, appearing on July 19 or 20 in Fig. 5. This means that the constant supplying rate of rain-water to the IV-stratum is $f_{\text{IVe}}=0.15$ mm/hr during the period of existence of the delayed interflow. The more detailed mechanism of the groundwater flow is left out because the storm runoff is being taken into account mainly in this paper.

(e) Model parameters with respect to the channel flow

The channel flow has two lateral inflow of the channel precipitation and the outflow resulting from slope process. Owing to the field observation, it is assumed that the width of the channel element catching directly rainfalls is 1.0 m and remains constant.

The configuration of the stream channel is very irregular and complicated. Accordingly, the so-called linear channel is assumed and the propagation speed for the

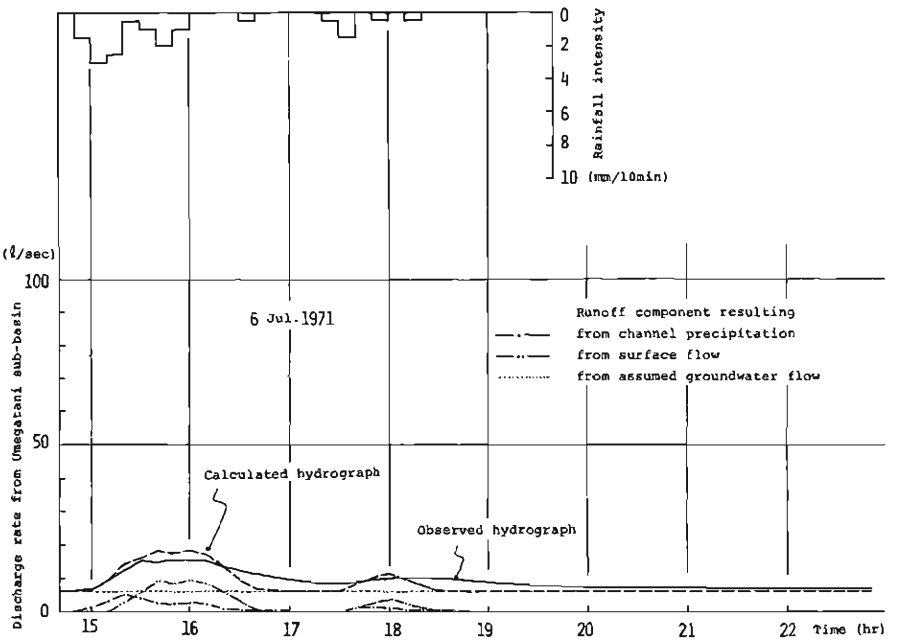

(a)

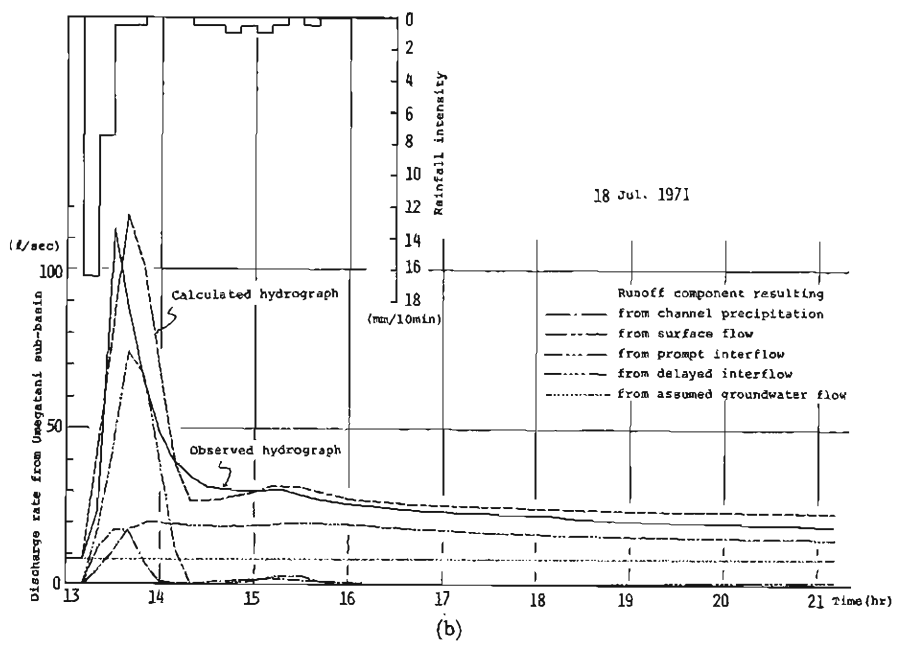

(b)

Fig. 13. Computational examples of hydrographs from the Umegatani sub-basin.
(a) July 6, 1971. (b) July 18, 1971.

channel flow is estimated to be 75 cm/sec, referring to the result of the velocity measurement by the salt method.

6. Computational examples of hydrographs in the sub-basin

Computational examples of the runoff hydrographs from the Umegatani sub-basin by the use of the runoff model presented in Section 4 and 5 are shown in Figs. 13 (a) and (b), in which the runoff component resulting from the groundwater flow at the beginning of the rainfall is assumed to remain unchanged during the short period of computation. In the case of Fig. 13 (a), there appear the runoff components resulting from only the surface flow as slope process and that from channel precipitation. In Fig. 13 (b), there appear appreciably the runoff components resulting from not only the surface flow but also the prompt and delayed interflows. The computed and observed hydrographs show a good agreement, nevertheless the values of parameters of this model are estimated by the results of observations at limited regions. Moreover, it is confirmed that a better agreement is obtained by the modification of the values of parameters concerned with the effective rainfall to the surface flow and f_{111c}.

As the intensity and cumulative amount of the rainfall become heavier and larger, usually, the water depth of the prompt interflow increases more and more until it exceeds the thickness of the II-stratum in the downstream part of the slope. When the water surface of prompt interflow appears on the top boundary of the II-stratum, there occurs the overland flow instead of the surface flow[6]. Therefore, the transition from surface flow to overland flow should be taken into account in the runoff model presented here, for extremely large rainfall.

As one of the conceptual runoff models, the so-called tank model has been proposed by Sugawara. Although the runoff model presented here consists of four strata to express slope process and is quite similar to the tank model composed by one series of four tanks, there is an essential difference among them. This is that the propagation process of rain-water is omitted in this original tank model. Recently, in order to express such a propagation process and a spacial variation of soil moisture, the tank model was improved to consist of four series of four tanks[7].

7. Formation process of runoff hydrograph in the stream net

The reasonable runoff model resulting from a heavy rainfall in a small watershed was constituted successfully, based upon the detailed observations of various hydrological events in the Umegatani sub-basin. In order to extrapolate such results to the whole experimental basin, the formation process of a runoff hydrograph through the stream net was discussed.

Generally, a watershed can be divided into many sub-basins which include only one link of stream net as introduced by Shreve[8] when a sub-basin specified is regarded as that of the lowest order. It is very normal to understand that the outer sub-basins divided have no essential difference between each other in the sense of storm runoff process. The inner sub-basins have the additional function of transmitting the inflow from an adjacent upper sub-basin to the outlet of the inner sub-basin. That is, the inner sub-basins can be regarded as the fields with the same function

as that of a outer sub-basin and the additional function of transmission of flood flow.

In order to examine the role of the stream channel in the formation process of runoff hydrograph under such considerations, let pick up, for example, the channel segment of order 3 together with the channel segments of just lower order attaching to the segment as shown in Fig. 14. Under the assumption of linear channel, the function of the channel segment of order 3 are to be divided into those of a channel through which the inflow at the inlet of the segment is transmitted to the outlet, and of a channel of order 2 which forms a stream net of a sub-basin of order 2 in company with remaining segments of order 1. After separating such a transmission function of the channel segment of highest order in an inner sub-basin, the runoff

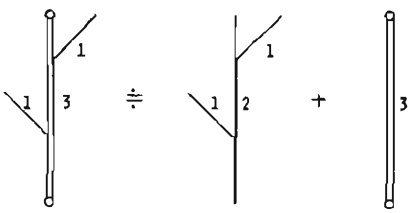

Fig. 14. The separation of the function of the main channel.

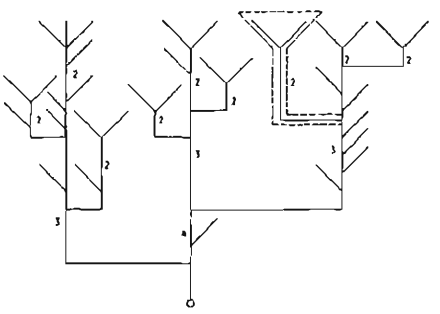

Fig. 15. The stream net of the basin.

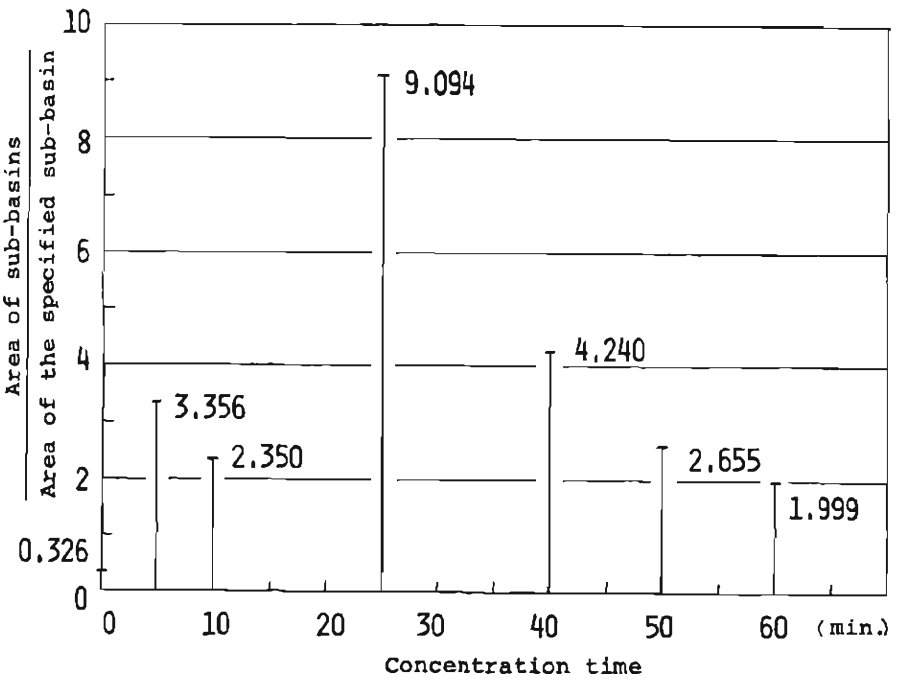

Fig. 16. The modified time-area-concentration diagram.

intensities from all the divided sub-basins can be assumed approximately to be proportional to their drainage area.

Applying such assumptions of separation and proportionality to a watershed under consideration, a modified time-area-concentration diagram can be obtained. Fig.16 is the modified time-area-concentration diagram for the experimental basin on the basis of the stream net shown in Fig. 15. In this diagram, the ordinate shows the area-ratio of a sub-basin to the Umegatani sub-basin and the abscissa the concentration time from the outlet of a sub-basin to the outlet of the whole basin. The large values of ordinate in this figure show the sum of area-ratios of the sub-basins which have a nearly equal concentration time. The propagation speed is assumed to remain constant in the whole stream net and to be 75 cm/sec obtained by the salt method.

The computational examples of the resultant hydrograph from the whole basin by the use of the modified time-area-concentration diagram given by Fig. 16 and of the hydrograph from the specified sub-basin are shown in Figs. 17 (a) and (b). In spite of the simple assumptions of linear superposition and propagation, the computed and observed hydrographs show a good agreement.

The understanding described here with respect to the role of the stream net in the formation process of a hydrograph in a watershed is very significant and applicable in solving the important problem of, for example, flood forecasting[9]. For the purpose of flood forecasting, the arrangement of raingauge stations in a watershed should be decided so as to be able to follow the formation process of a runoff hydrograph resulting from a storm rainfall in the watershed. And the general theory

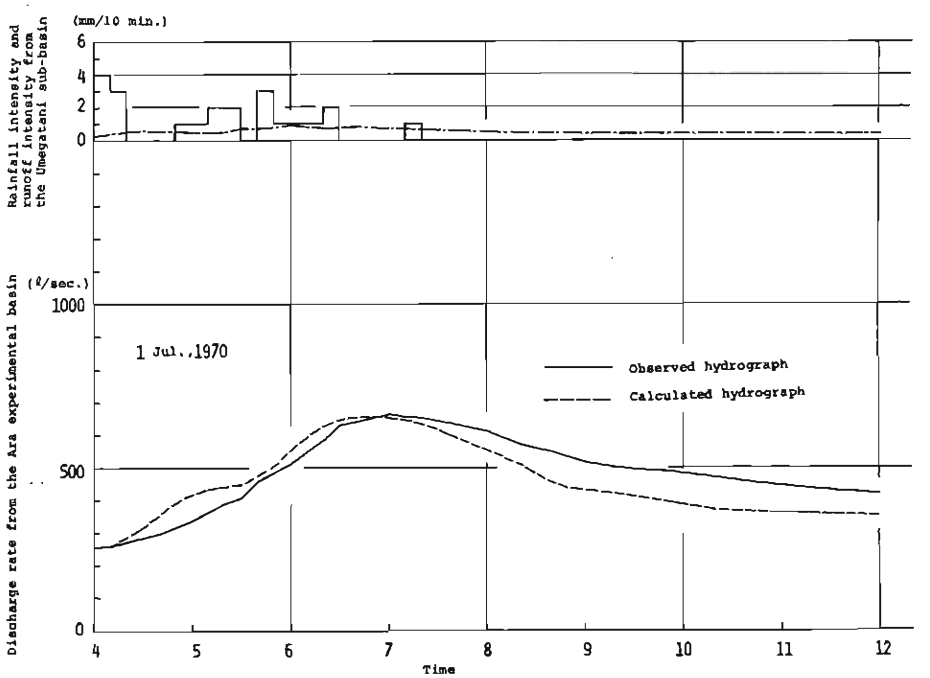

(a)

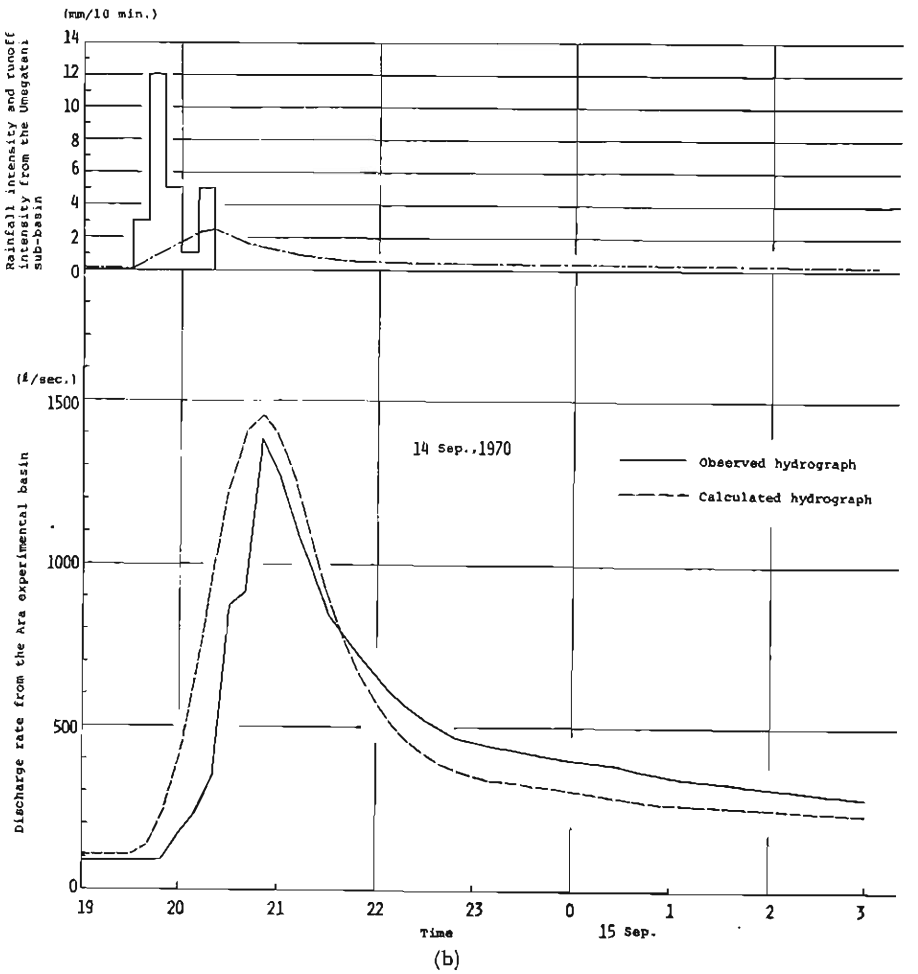

(b)

Fig. 17. Computational examples of hydrographs from the whole basin.
(a) July 1, 1970. (b) September 14, 1970.

expressing the magnitude and lag time of a flood peak can be derived by analysing the formation process of a flood hydrograph in the common type of stream net under the assumption presented above[10].

8. Conclusion

In order to elucidate the runoff process, detailed observations of the hydrological phenomena were carried out in the Ara experimental basin. On the basis of observational results of surface flow, soil moisture, seeping water from a rock fissure, we constructed the runoff model having four strata for slope process and one stream reach for channel process for a small watershed. For each stratum, the intial loss could be calculated by the cummulative evapotranspiration curve obtained by the method of water balance, and infiltration rate was estimated by the help of the

observational result of seeping water from the fissure of a rock. The calculated hydrographs using the model show a good agreement with the observed ones.

Next, formation process of runoff hydrograph in the stream net was studied by the modified time-area-concentration diagram based on the simple assumptions of linear superposition and propagation, and the calculated hydrographs give good results.

Finally, two runoff models developed in this paper, the storm runoff model for a small watershed and the formation model of flood hydrograph for a large watershed, include the physical characteristics of the watershed faithfully and so every hydrological event occurring in the watershed is simulated in it. Man's effect on runoff process, for example the construction of residence area by cutting off a hill area and river training, may be evaluated and predictions made by applying these runoff models.

Acknowledgement

The data of the runoff at the outlet of the whole basin are by courtesy of Prof. T. Maruyama, the Department of Agriculture Engineering, Kyoto University.

References

1) Ishihara, Y. and Kobatake, S.: Occurrence of direct runoff in mountain area, Annuals of Disaster Prevention Research Institute, Kyoto University, Vol. 12B, 1969, pp. 247–259 (in Japanese)
2) Ishihara, Y. and Kobatake, S.: On the water balance in Ara experimental basin, Annuals of Disaster Prevention Research Institute, Kyoto University, Vol. 14B, 1971, pp. 131–141, (in Japanese)
3) Ishihara, Y. and Kobatake, S.: On the water balance in Ara experimental basin(2), Annuals of Disaster Prevention Research Institute, Kyoto University, Vol. 15B, 1972, (in
4) Japanese) Ishihara, Y. and Kobatake, S.: Relation between runoffs from small and large river basins, Annuals of Disaster Prevention Research Institute, Kyoto University, Vol. 17B, 1974, pp. 471–478 (in Japanese)
5) Ishihara, Y. and Kobatake, S.: Initial storage of rain-water in runoff process, — Interception by trees — , Annuals of Disaster Prevention Research Institute, Kyoto University, Vol. 13B, pp. 69–81 (in Japanese)
6) Ishihara, T., Ishihara, Y., Takasao, T. and Rai, C.: Study on the characteristics of flood in Yura River, Annuals of Disaster Prevention Research Institute, Kyoto University, Vol. 5A, 1962, pp. 147–173 (in Japanese)
7) Sugawara, M., Ozaki, E., Watanabe, I. and Katsuyama, Y.: Tank model and its application to Bird Creek, Wollombi Brook, Bikin River, Kitsu River, Sanaga River and Nam Mune, Research notes of the National Research Center for Disaster Prevention, No. 11, 1974.
8) Smart, J. S.: Channel network, In Advances in Hydroscience (edited by V. T. Chow), Vol. 8, 1972, pp. 305–345, Academic Press
9) Ishihara, T. and Ishihara, Y.: Operational arrangement of raingauge stations in forecasting flash floods, Proceedings of the Paris Symposium, IAHS–AISH Publ. No. 112, 1974
10) Ishihara, Y. and Sato, M.: Specific discharge of flood peak, Annuals of Disaster Prevention Research Institute, Kyoto University, Vol. 18B, 1975, pp. 415–423 (in Japanese)